Eur. Phys. J. C (2021) 81:97
https://doi.org/10.1140/epjc/s10052-021-08915-1

THE EUROPEAN PHYSICAL JOURNAL C

Check for updates

Regular Article - Theoretical Physics

Energy map and effective metric in an effective-one-body theory based on the second-post-Minkowskian approximation

Xiaokai He[1,2,a], **Manman Sun**[1,b], **Jiliang Jing**[1,c], **Zhoujian Cao**[3,d]

[1] Department of Physics, Key Laboratory of Low Dimensional Quantum Structures and Quantum Control of Ministry of Education, and Synergetic Innovation Center for Quantum Effects and Applications, Hunan Normal University, Changsha 410081, Hunan, People's Republic of China
[2] School of Mathematics and Computational Science, Hunan First Normal University, Changsha 410205, People's Republic of China
[3] Department of Astronomy, Beijing Normal University, Beijing 100875, People's Republic of China

Received: 5 November 2020 / Accepted: 24 January 2021 / Published online: 30 January 2021
© The Author(s) 2021

Abstract Effective-one-body (EOB) theory was originally proposed based on the post-Newtonian (PN) approximation and plays an important role in the analysis of gravitational wave signals. Recently, the post-Minkowskian (PM) approximation has been applied to the EOB theory. The energy map and the effective metric are the two key building blocks of the EOB theory, and in PN approximation radial action variable correspondence is employed to construct the energy map and the effective metric. In this paper, we employ the PM approximation up to the second order, and use the radial action variable correspondence and the precession angle correspondence to construct the energy map and the effective metric. We find that our results based on the radial action variable correspondence, are exactly the same with those obtained based on the precession angle correspondence. Furthermore, we compare the results obtained in this work to the previous existing ones.

1 Introduction

Since the first direct detection of gravitational waves (GW) by LIGO [1], more than 50 GW detection events have been confirmed [2–6]. The era of gravitational wave astronomy is coming and it can be used as a powerful tool to investigate gravitational physics [7]. In the success of GW detection, the gravitational waveform template, which is an essential part of the matched filtering technique, plays a very important role. To construct gravitational waveform template, the theoretical models of gravitational radiation are necessary. Among several existing theoretical models, the effective-one-body-numerical-relativity (EOBNR) has been widely used in practical GW detection [7–10].

Currently, the EOBNR model is a combination of effective-one-body (EOB) theory and numerical relativity (NR) [9]. The EOB theory, which is inspired by the electromagnetically interacting quantum two-body problem [11], has been applied to compute the gravitational waveform emitted by binary black holes [11–14]. The original EOB theory is based on post-Newtonian (PN) approximation, and the basic idea is to map the real two-body problem to an effective one body problem. More precisely, the EOB formalism consists of two main parts: the conservative dynamics part and the radiation reaction part. The conservative dynamics of a two-body system is described by an effective Hamiltonian. To build the relations between the real two-body system and the effective-one-body system, the energy map between the real relativistic energy $\mathcal{E}$ (in the center of mass frame) and the effective one $\mathcal{E}_0$ is essential. Similar to the Bohr–Sommerfeld quantization conditions of bound states in quantum mechanics, the energy map can be obtained by identifying the real radial action variable I_R to the effective one I_R^0. Consequently, the energy map

$$f : \mathcal{E} \to \mathcal{E}_0, \tag{1.1}$$

can be expressed as a PN expansion series [11]

$$\frac{\mathcal{E}_0^{\rm nr}}{m_0c^2} = \frac{\mathcal{E}_{\rm real}^{\rm nr}}{\mu c^2}\left[1+\alpha_1\left(\frac{\mathcal{E}_{\rm real}^{\rm nr}}{\mu c^2}\right)+\alpha_2\left(\frac{\mathcal{E}_{\rm real}^{\rm nr}}{\mu c^2}\right)^2 +\alpha_3\left(\frac{\mathcal{E}_{\rm real}^{\rm nr}}{\mu c^2}\right)^3+\alpha_4\left(\frac{\mathcal{E}_{\rm real}^{\rm nr}}{\mu c^2}\right)^4+\cdots\right], \tag{1.2}$$

with

[a] e-mail: hexiaokai77@163.com
[b] e-mail: sunmanman@smail.hunnu.edu.cn
[c] e-mail: jljing@hunnu.edu.cn (corresponding author)
[d] e-mail: zjcao@amt.ac.cn

$$\mathcal{E}_0^{\rm nr} = \mathcal{E}_0 - m_0c^2,$$
$$\mathcal{E}_{\rm real}^{\rm nr} = \mathcal{E} - (m_1+m_2)c^2,$$
$$\mu = \frac{m_1m_2}{m_1+m_2}, \tag{1.3}$$

where m_1, m_2 are the masses of the real two-body system, m_0 is the mass of the effective particle and 'nr' means non-relativistic. It is striking that the energy map, at the 4PN order, exhibits a very simple structure [15]

$$\alpha_1 = \frac{\nu}{2},\ \alpha_2 = \alpha_3 = \alpha_4 = 0, \tag{1.4}$$

where

$$\nu = \frac{m_1m_2}{(m_1+m_2)^2} \tag{1.5}$$

is the symmetric mass ratio. By substituting the above strikingly simple formula into the relativistic real energy $\mathcal{E}$ and the effective energy $\mathcal{E}_0$, the energy map (1.2) at the 4PN order becomes

$$\frac{\mathcal{E}_0}{m_0c^2} = \frac{\mathcal{E}^2 - m_1^2c^4 - m_2^2c^4}{2m_1m_2c^4}. \tag{1.6}$$

In 2016, Damour investigated the energy map based on post-Minkowskian (PM) approximation [16]. Different to the PN approach in which $\frac{v}{c}$ is assumed to be small, the PM approach uses the gravitational constant G as an expansion parameter and $\frac{v}{c}$ is not required to be small any more [17,18]. Damour considered a scattering state of a two-body system [16] and calculated the real two-body scattering function $\chi_{\rm 1PM}^{\rm real}$ and the effective-one-body scattering function $\chi_{\rm 1PM}^{\rm eff}$ at the 1PM approximation. By identifying $\chi_{\rm 1PM}^{\rm real}$ and $\chi_{\rm 1PM}^{\rm eff}$, he found that the energy map between the real two-body energy $\mathcal{E}$ and the energy $\mathcal{E}_0$ of the effective particle takes the form as Eq. (1.6) at 1PM order. Since PM approximation does not assume $\frac{v}{c}$ is small, this means Eq. (1.6) is valid for all orders of $\frac{v}{c}$.

In 2017, Bini and Damour studied the gravitational spin-orbit coupling of a binary system at the 1PM order [19], and they extended the results to the 2PM order later [20]. Based on the scattering "spin holonomy", they showed the energy map obtained in Ref. [16] still holds at the 2PM order. In addition, they calculated the two gyrogravitomagnetic ratios which is adopted to describe the spin-orbit coupling in the EOB formalism. But they did not give the explicit expression of effective metric at the 2PM order [19,20]. The PM approximation has attracted great attention in recent years. For example, the structure properties and the scattering of tidally interacting bodies in PM approximation are discussed [21,22], and see Refs. [22–37], for more information on this direction.

In 2018, Damour found a 2PM effective Hamiltonian based on the calculation of scattering angles [38]. A generalized mass-shell condition, which contains a Finsler-type contribution has been used in such an effective Hamiltonian. Along this way, Antonelli et al extended the 2PM effective Hamiltonian to the 3PM order and discussed the binding energy of a two-body system [39].

In order to construct gravitational waveform model for compact binary objects coalescence, a bound state instead of a scattering state is needed. An interesting question is whether the PM effective Hamiltonian can be derived from a bound state. Since the Finsler-type term in the related Hamiltonian [38] is introduced artificially, another interesting question is whether the PM effective Hamiltonian can be derived without using the Finsler-type term. In this paper, we answer these two questions up to the 2PM order. We show that the energy map (1.6) still holds for bound state, and construct the effective metric at the 2PM order. Two independent methods are used to construct the effective metric: one is based on the calculation of the action variables of the real two-body system and the EOB system, and the other one is based on the calculation of the precession angle.

The rest of the paper is organized as follows. In Sect. 2, we compute the radial action variable I_R from the 2PM Hamiltonian of the real two-body system. Then the effective radial action variable I_R^0 of a test particle moving in a deformed Schwarzschild spacetime (effective background spacetime) is calculated at the 2PM order. Based on these results, the energy map between the real relativistic energy $\mathcal{E}$ of a two-body system and the effective relativistic energy $\mathcal{E}_0$ of the EOB system are obtained, and the effective metric is derived. In Sect. 3, we get the effective metric at the 2PM order by calculating and comparing the precession angle of a real two-body system and the EOB system. We find that the results are consistent to those obtained in Sect. 2. In Sect. 4, we compare our 2PM effective Hamiltonian with the existing results and show that all the results are consistent at 3PN accuracy. At last, summary and discussion are given in Sect. 5.

We use the unit with $c = 1$ throughout the paper, which is suitable for calculations within the PM framework.

2 Energy map and effective metric based on action variable

In this section, we first calculate the action variable both for a two-body system and the EOB system at 2PM order, respectively. By identifying the action variables, the energy map and the effective metric in EOB theory are then constructed.

2.1 Radial action variable of a two-body system at 2PM order

In 2019, it was shown by Bern et al. [31,32] that the conservative Hamiltonian of a massive spinless binary system at the 2PM approximation can be expressed explicitly as

$$
\begin{aligned}
H_{\rm 2PM} =& \sqrt{\vec{p}^2+m_1^2}+\sqrt{\vec{p}^2+m_2^2}+\frac{m_1^2m_2^2G}{\sqrt{\vec{p}^2+m_1^2}\sqrt{\vec{p}^2+m_2^2}r}\left(1-\frac{2\left(\vec{p}^2+\sqrt{\vec{p}^2+m_1^2}\sqrt{\vec{p}^2+m_2^2}\right)^2}{m_1^2m_2^2}\right)+\frac{m_1^2m_2^2(m_1+m_2)G^2}{\sqrt{\vec{p}^2+m_1^2}\sqrt{\vec{p}^2+m_2^2}r^2}\\
&\times\left[\frac{3}{4}\left(1-\frac{5\left(\vec{p}^2+\sqrt{\vec{p}^2+m_1^2}\sqrt{\vec{p}^2+m_2^2}\right)^2}{m_1^2m_2^2}\right)-\frac{4\left(\sqrt{\vec{p}^2+m_1^2}+\sqrt{\vec{p}^2+m_2^2}\right)\left(\vec{p}^2+\sqrt{\vec{p}^2+m_1^2}\sqrt{\vec{p}^2+m_2^2}\right)}{(m_1+m_2)\sqrt{\vec{p}^2+m_1^2}\sqrt{\vec{p}^2+m_2^2}}\right.\\
&\times\left(1-\frac{2(\vec{p}^2+\sqrt{\vec{p}^2+m_1^2}\sqrt{\vec{p}^2+m_2^2})^2}{m_1^2m_2^2}\right)-\frac{\left(m_1^2+m_2^2+2\vec{p}^2+\sqrt{\vec{p}^2+m_1^2}\sqrt{\vec{p}^2+m_2^2}\right)}{2m_1^2m_2^2(m_1+m_2)(\vec{p}^2+m_1^2)(\vec{p}^2+m_2^2)\left(\sqrt{\vec{p}^2+m_1^2}+\sqrt{\vec{p}^2+m_2^2}\right)}\cdot\\
&\left.\times\left(m_1^2\left(2\vec{p}^2+m_2^2\right)+2\vec{p}^2\left(m_2^2+2\left(\vec{p}^2+\sqrt{\vec{p}^2+m_1^2}\sqrt{\vec{p}^2+m_2^2}\right)\right)\right)^2\right].
\end{aligned}
\tag{2.1}
$$

Based on the above Hamiltonian (2.1), the radial action can be calculated. Within a spherical coordinate system $\{r,\theta,\phi\}$, we have

$$
\begin{aligned}
\vec{p}^2 &= p_r^2+\frac{p_\theta^2}{r^2}+\frac{p_\phi^2}{r^2\sin^2\theta},\\
\vec{r}\cdot\vec{p} &= rp_r,\\
\vec{p}^2\vec{r}^2-(\vec{r}\cdot\vec{p})^2 &= p_\theta^2+\frac{p_\phi^2}{\sin^2\theta},
\end{aligned}
\tag{2.2}
$$

which implies that there are two conservative quantities, i.e. the energy $\mathcal{E}$ and the angular momentum $J=p_\phi$. Due to the conservative quantity J, the orbit is restricted in a plane. Without loss of generality, we set $\theta=\frac{\pi}{2}$. The reduced Hamiltonian in the equatorial ($\theta=\frac{\pi}{2}$) plane becomes

$$
\begin{aligned}
H_{\rm 2PM} =& \sqrt{p_r^2+\frac{J^2}{r^2}+m_1^2}+\sqrt{p_r^2+\frac{J^2}{r^2}+m_2^2}+\frac{m_1^2m_2^2G}{\sqrt{p_r^2+\frac{J^2}{r^2}+m_1^2}\sqrt{p_r^2+\frac{J^2}{r^2}+m_2^2}r}\\
&\times\left(1-\frac{2\left(p_r^2+\frac{J^2}{r^2}+\sqrt{p_r^2+\frac{J^2}{r^2}+m_1^2}\sqrt{p_r^2+\frac{J^2}{r^2}+m_2^2}\right)^2}{m_1^2m_2^2}\right)+\frac{m_1^2m_2^2(m_1+m_2)G^2}{\sqrt{p_r^2+\frac{J^2}{r^2}+m_1^2}\sqrt{p_r^2+\frac{J^2}{r^2}+m_2^2}r^2}\\
&\times\left[\frac{3}{4}\left(1-\frac{5\left(p_r^2+\frac{J^2}{r^2}+\sqrt{p_r^2+\frac{J^2}{r^2}+m_1^2}\sqrt{p_r^2+\frac{J^2}{r^2}+m_2^2}\right)^2}{m_1^2m_2^2}\right)\right.\\
&-\frac{4\left(\sqrt{p_r^2+\frac{J^2}{r^2}+m_1^2}+\sqrt{p_r^2+\frac{J^2}{r^2}+m_2^2}\right)\left(p_r^2+\frac{J^2}{r^2}+\sqrt{p_r^2+\frac{J^2}{r^2}+m_1^2}\sqrt{p_r^2+\frac{J^2}{r^2}+m_2^2}\right)}{(m_1+m_2)\sqrt{p_r^2+\frac{J^2}{r^2}+m_1^2}\sqrt{p_r^2+\frac{J^2}{r^2}+m_2^2}}\cdot\\
&\times\left(1-\frac{2\left(p_r^2+\frac{J^2}{r^2}+\sqrt{p_r^2+\frac{J^2}{r^2}+m_1^2}\sqrt{p_r^2+\frac{J^2}{r^2}+m_2^2}\right)^2}{m_1^2m_2^2}\right)\\
&-\frac{\left(m_1^2+m_2^2+2\left(p_r^2+\frac{J^2}{r^2}\right)+\sqrt{p_r^2+\frac{J^2}{r^2}+m_1^2}\sqrt{p_r^2+\frac{J^2}{r^2}+m_2^2}\right)}{2m_1^2m_2^2(m_1+m_2)\left(p_r^2+\frac{J^2}{r^2}+m_1^2\right)\left(p_r^2+\frac{J^2}{r^2}+m_2^2\right)\left(\sqrt{p_r^2+\frac{J^2}{r^2}+m_1^2}+\sqrt{p_r^2+\frac{J^2}{r^2}+m_2^2}\right)}\cdot\\
&\left.\times\left(m_1^2\left(2\left(p_r^2+\frac{J^2}{r^2}\right)+m_2^2\right)+2\left(p_r^2+\frac{J^2}{r^2}\right)\left(m_2^2+2\left(p_r^2+\frac{J^2}{r^2}+\sqrt{p_r^2+\frac{J^2}{r^2}+m_1^2}\sqrt{p_r^2+\frac{J^2}{r^2}+m_2^2}\right)\right)\right)^2\right].
\end{aligned}
\tag{2.3}
$$

We use the Hamilton–Jacobi approach to solve the 2PM dynamics. In polar coordinates, the reduced action is

$$S = -\mathcal{E}t + J\phi + S_r(r, \mathcal{E}, J). \tag{2.4}$$

Then the Hamilton–Jacobi equation

$$\frac{\partial S}{\partial t} + H\left(q, \frac{\partial S}{\partial q}\right) = 0, \tag{2.5}$$

becomes

$$\begin{aligned}
\mathcal{E} = {} & \sqrt{p_r^2 + \frac{J^2}{r^2} + m_1^2} + \sqrt{p_r^2 + \frac{J^2}{r^2} + m_2^2} + \frac{m_1^2 m_2^2 G}{\sqrt{p_r^2 + \frac{J^2}{r^2} + m_1^2}\sqrt{p_r^2 + \frac{J^2}{r^2} + m_2^2}\, r} \\
& \times \left(1 - \frac{2\left(p_r^2 + \frac{J^2}{r^2} + \sqrt{p_r^2 + \frac{J^2}{r^2} + m_1^2}\sqrt{p_r^2 + \frac{J^2}{r^2} + m_2^2}\right)^2}{m_1^2 m_2^2}\right) \\
& + \frac{m_1^2 m_2^2 (m_1 + m_2) G^2}{\sqrt{p_r^2 + \frac{J^2}{r^2} + m_1^2}\sqrt{p_r^2 + \frac{J^2}{r^2} + m_2^2}\, r^2}\left[\frac{3}{4}\left(1 - \frac{5\left(p_r^2 + \frac{J^2}{r^2} + \sqrt{p_r^2 + \frac{J^2}{r^2} + m_1^2}\sqrt{p_r^2 + \frac{J^2}{r^2} + m_2^2}\right)^2}{m_1^2 m_2^2}\right)\right. \\
& \left. - \frac{4\left(\sqrt{p_r^2 + \frac{J^2}{r^2} + m_1^2} + \sqrt{p_r^2 + \frac{J^2}{r^2} + m_2^2}\right)\left(p_r^2 + \frac{J^2}{r^2} + \sqrt{p_r^2 + \frac{J^2}{r^2} + m_1^2}\sqrt{p_r^2 + \frac{J^2}{r^2} + m_2^2}\right)}{(m_1 + m_2)\sqrt{p_r^2 + \frac{J^2}{r^2} + m_1^2}\sqrt{p_r^2 + \frac{J^2}{r^2} + m_2^2}}\right. \\
& \times \left(1 - \frac{2\left(p_r^2 + \frac{J^2}{r^2} + \sqrt{p_r^2 + \frac{J^2}{r^2} + m_1^2}\sqrt{p_r^2 + \frac{J^2}{r^2} + m_2^2}\right)^2}{m_1^2 m_2^2}\right) \\
& - \frac{\left(m_1^2 + m_2^2 + 2\left(p_r^2 + \frac{J^2}{r^2}\right) + \sqrt{p_r^2 + \frac{J^2}{r^2} + m_1^2}\sqrt{p_r^2 + \frac{J^2}{r^2} + m_2^2}\right)}{2m_1^2 m_2^2 (m_1 + m_2)\left(p_r^2 + \frac{J^2}{r^2} + m_1^2\right)\left(p_r^2 + \frac{J^2}{r^2} + m_2^2\right)\left(\sqrt{p_r^2 + \frac{J^2}{r^2} + m_1^2} + \sqrt{p_r^2 + \frac{J^2}{r^2} + m_2^2}\right)} \\
& \left. \times \left(m_1^2\left(2(p_r^2 + \frac{J^2}{r^2}) + m_2^2\right) + 2\left(p_r^2 + \frac{J^2}{r^2}\right)\left(m_2^2 + 2\left(p_r^2 + \frac{J^2}{r^2} + \sqrt{p_r^2 + \frac{J^2}{r^2} + m_1^2}\sqrt{p_r^2 + \frac{J^2}{r^2} + m_2^2}\right)\right)\right)^2\right].
\end{aligned} \tag{2.6}$$

Now we solve $p_r (\equiv \frac{dS_r}{dr})$ from Eq. (2.6). Following the prescriptions given in Ref. [32], we expand p_r^2 as

$$p_r^2 = \frac{P_0 r^2 - J^2}{r^2} + P_1\left(\frac{G}{r}\right) + P_2\left(\frac{G}{r}\right)^2 + \cdots. \tag{2.7}$$

Plugging Eq. (2.7) into Eq. (2.6), we obtain

$$P_0 = \frac{\mathcal{E}^4 + (m_1^2 - m_2^2)^2 - 2\mathcal{E}^2(m_1^2 + m_2^2)}{4\mathcal{E}^2}, \tag{2.8}$$

$$P_1 = \frac{\mathcal{E}^4 - 2\mathcal{E}^2(m_1^2 + m_2^2) + (m_1^4 + m_2^4)}{\mathcal{E}}, \tag{2.9}$$

and

$$P_2 = \frac{3(m_1 + m_2)}{8\mathcal{E}}\Big(5\mathcal{E}^4 + 5m_1^4 + 5m_2^4 + 6m_1^2 m_2^2 - 10\mathcal{E}^2(m_1^2 + m_2^2)\Big). \tag{2.10}$$

According to the Hamilton–Jacobi theory, the radial effective potential $\mathcal{R}(r, \mathcal{E}, J)$ at the 2PM order reads

$$\mathcal{R}(r, \mathcal{E}, J) = \frac{P_0 r^2 - J^2}{r^2} + P_1\left(\frac{G}{r}\right) + P_2\left(\frac{G}{r}\right)^2. \tag{2.11}$$

From definition of the radial action variable [11]

$$I_R \equiv \frac{2}{2\pi}\int_{r_{\min}}^{r_{\max}} dr\sqrt{\mathcal{R}(r, \mathcal{E}, J)}, \tag{2.12}$$

where the turning points of the effective potential $\mathcal{R}(r, \mathcal{E}, J)$ $r_{\min}$ and $r_{\max}$ are given by

$$\begin{aligned}
r_{\min} &= \frac{-P_1 G + \sqrt{P_1^2 G^2 - 4P_0 P_2 G^2 + 4P_0 J^2}}{2P_0}, \\
r_{\max} &= \frac{-P_1 G - \sqrt{P_1^2 G^2 - 4P_0 P_2 G^2 + 4P_0 J^2}}{2P_0},
\end{aligned} \tag{2.13}$$

one obtains

$$\int_{r_{\min}}^{r_{\max}}\left[\frac{P_0 r^2-J^2}{r^2}+P_1\left(\frac{G}{r}\right)+P_2\left(\frac{G}{r}\right)^2\right]^{1/2}dr = \left(\frac{P_1}{2\sqrt{-P_0}}-\sqrt{J^2-P_2G^2}\right)\pi. \tag{2.14}$$

Putting Eq. (2.11) into Eq. (2.12), together with Eqs. (2.8), (2.9), (2.10) and (2.14), we obtain the explicit expression of the radial action variable of the real two-body system at the 2PM order as

$$I_R = -J+\frac{(\mathcal{E}^4+m_1^4+m_2^4-2\mathcal{E}^2(m_1^2+m_2^2))G}{\sqrt{-\mathcal{E}^4+2(m_1^2+m_2^2)\mathcal{E}^2-(m_1^2-m_2^2)^2}} +\frac{3(m_1+m_2)G^2}{16\mathcal{E}J}\Big(5\mathcal{E}^4+5m_1^2+5m_2^2 +6m_1^2m_2^2-10\mathcal{E}^2(m_1^2+m_2^2)\Big). \tag{2.15}$$

2.2 Radial action variable of the EOB system at 2PM order

In this subsection, we calculate the effective radial action variable I_R^0, which is deduced from the dynamics of a test particle with rest mass m_0 moving in an effective curved background spacetime with metric $g_{\mu\nu}^{\text{eff}}$. Following the spirit of EOB approach [11,16], the effective metric which corresponds to a spinless two-body system is given by

$$ds_{\text{eff}}^2 = -A(R)dt^2+B(R)dR^2 +C(R)R^2(d\Theta^2+\sin^2\Theta d\Phi^2). \tag{2.16}$$

At the second order in G, $A(R)$ and $B(R)$ can be expanded as

$$A(R)=1-\frac{2GM_0}{R}+a_2\left(\frac{GM_0}{R}\right)^2, \tag{2.17}$$

$$B(R)=1+\beta_1\frac{2GM_0}{R}+b_2\left(\frac{GM_0}{R}\right)^2, \tag{2.18}$$

where β_1, a_2, b_2 are dimensionless parameters and M_0 is a mass parameter which denotes the the mass of the effective background [16]. The function $C(R)$ may be fixed either to $C(R)=1$ in Schwarzschild coordinates or to $C(R)=B(R)$ in isotropic coordinates.

For a test particle moving in the effective background spacetime, the effective Hamilton–Jacobi equation reads

$$g_{\text{eff}}^{\mu\nu}\frac{\partial S_{\text{eff}}}{\partial x^\mu}\frac{\partial S_{\text{eff}}}{\partial x^\nu}+m_0^2=0. \tag{2.19}$$

In the equatorial plane ($\Theta=\frac{\pi}{2}$), S_{eff} reduces to

$$S_{\text{eff}}=-\mathcal{E}_0 t+J_0\Phi+S_R^0(R,\mathcal{E},J_0), \tag{2.20}$$

where $\mathcal{E}_0$ and J_0 are the effective energy and the angular momentum, respectively.

By substituting Eq. (2.20) into Eq. (2.19), we obtain

$$\frac{dS_R^0}{dR}=\sqrt{\mathcal{R}_0(R,\mathcal{E}_0,J_0)}, \tag{2.21}$$

where

$$\mathcal{R}_0(R,\mathcal{E}_0,J_0)=\frac{B(R)}{A(R)}\mathcal{E}_0^2-B(R)\left(m_0^2+\frac{J_0^2}{C(R)R^2}\right). \tag{2.22}$$

Based on the definition of the effective radial action variable $I_R^0(\mathcal{E}_0,J_0)$

$$I_R^0(\mathcal{E}_0,J_0)=\frac{2}{2\pi}\int_{R_{\min}}^{R_{\max}}dR\sqrt{\mathcal{R}_0(R,\mathcal{E}_0,J_0)}, \tag{2.23}$$

we calculate the effective radial action variable $I_R^0(\mathcal{E}_0,J_0)$ both in the Schwarzschild and in the isotropic gauges in the following.

2.2.1 Action variable in the Schwarzschild gauge

For this case, $C(R)=1$. By substituting Eqs. (2.17) and (2.18) into Eq. (2.22), and letting a_2, β_1 and b_2 as expansion coefficients, we get

$$\mathcal{R}_0(R,\mathcal{E}_0,J_0)=\hat{A}+\frac{2\hat{B}}{R}+\frac{\hat{C}}{R^2}+\frac{\hat{D}_1}{R^3}+\frac{\hat{D}_2}{R^4}, \tag{2.24}$$

where

$$\begin{aligned}\hat{A}&=\mathcal{E}_0^2-m_0^2,\\ \hat{B}&=GM_0(-m_0^2\beta_1+\mathcal{E}_0^2(1+\beta_1)),\\ \hat{C}&=-J_0^2-b_2G^2m_0^2M_0^2\\ &\quad+\mathcal{E}^2G^2M_0^2(4-a_2+b_2+4\beta_1),\\ \hat{D}_1&=-2M_0\beta_1J_0^2G,\\ \hat{D}_2&=-b_2G^2J_0^2M_0^2.\end{aligned} \tag{2.25}$$

In general, it is hard to get the exact expression of $I_R^0(\mathcal{E}_0,J_0)$ by direct calculation. Fortunately, there exists a simpler way to obtain $I_R^0(\mathcal{E}_0,J_0)$ which does not need to consider the explicit value of the turning points $r_{\min}$ and $r_{\max}$. If

$$I=\frac{2}{2\pi}\int_{r_{\min}}^{r_{\max}}dr\left(A+\frac{2B}{r}+\frac{C}{r^2}+\frac{D_1}{r^3}+\frac{D_2}{r^4}+\frac{D_3}{r^5}\right)^{\frac{1}{2}} \tag{2.26}$$

where $A<0$, $B>0$, $C<0$, $D_1=\mathcal{O}(\epsilon)$, D_2 and $D_3=\mathcal{O}(\epsilon^2)$, we have [40]

$$I=\frac{B}{\sqrt{-A}}-\sqrt{-C}\Bigg[1-\frac{1}{2}\frac{B}{C^2}\left(D_1-\frac{3}{2}\frac{BD_2}{C}+\frac{15}{8}\frac{D_1^2B}{C^2}\right)-\frac{1}{4}\frac{A}{C^2}\left(D_2-\frac{3}{4}\frac{D_1^2}{C}\right)+\frac{3}{4}\frac{B}{C^3}\left(A-\frac{5}{3}\frac{B^2}{C}\right)D_3\Bigg]+\mathcal{O}(\epsilon^3). \tag{2.27}$$

Using Eq. (2.27), the effective radial action variable $I_R^0(\mathcal{E}_0, J_0)$ at the second order in G turns into

$$I_R^0(\mathcal{E}_0,J_0)=-J_0+\frac{M_0G(-m_0^2\beta_1+(1+\beta_1)\mathcal{E}_0^2)}{\sqrt{-\mathcal{E}_0^2+m_0^2}}+\frac{M_0^2G^2}{4J_0}\Big[\mathcal{E}_0^2(8-2a_2+b_2+4\beta_1-\beta_1^2)+m_0^2(\beta_1^2-b_2)\Big]. \tag{2.28}$$

2.2.2 Action variable in the isotropic gauge

For this case, $C(R)=B(R)$. Following the same procedures shown in the above, we get

$$I_R^0(\mathcal{E}_0,J_0)=-J_0+\frac{M_0G((1+\tilde{\beta}_1)\mathcal{E}_0^2-\tilde{\beta}_1m_0^2)}{\sqrt{-\mathcal{E}_0^2+m_0^2}}+\frac{M_0^2G^2(\mathcal{E}_0^2(4-\tilde{a}_2+\tilde{b}_2+4\tilde{\beta}_1)-m_0^2\tilde{b}_2)}{2J_0}. \tag{2.29}$$

By comparing Eq. (2.28) with Eq. (2.29), we obtain

$$\begin{aligned}\tilde{\beta}_1&=\beta_1,\\ \tilde{a}_2&=a_2+2\beta_1,\\ \tilde{b}_2&=\frac{b_2}{2}-\frac{\beta_1^2}{2}.\end{aligned} \tag{2.30}$$

which is consistent with the results given in Ref. [11].

2.3 Energy map and effective metric at the 2PM order

In this subsection, we investigate the relations between the EOB system and the real two-body system. Especially, we show that the energy map between the two systems is consistent to the one given in the Ref. [16]. We would like to emphasize that the energy map in [16] was deduced by investigating the scattering angle while here we use the radial action variable or precession angle. Moreover, the effective background metric is constructed at the 2PM order.

A natural and physical choice of the relations between EOB quantities and real two-body ones are [11,16]

$$m_0=\frac{m_1m_2}{m_1+m_2}, \tag{2.31}$$

$$M_0=m_1+m_2. \tag{2.32}$$

Moreover, following the Ref. [11], we choose

$$\beta_1=1 \tag{2.33}$$

which means the effective metric coincides with the linearized Schwarzschild metric with $M_0=m_1+m_2$.

Inspired by the Bohr–Sommerfeld quantization conditions, we adopt the following identification of the effective radial action variable I_R^0 and the real two-body one I_R:

$$I_R^0(\mathcal{E}_0,J_0)=I_R(\mathcal{E},J). \tag{2.34}$$

By combining Eqs. (2.15), (2.28), (2.31), (2.32), (2.33) and (2.34), we can get the energy map

$$\mathcal{E}_0=f[\mathcal{E}]. \tag{2.35}$$

More precisely, the 0th-order (in G) of the Eq. (2.34) gives

$$J_0=J. \tag{2.36}$$

The 1st-order of the Eq. (2.34) yields

$$\mathcal{E}_0=\frac{\mathcal{E}^2-m_1^2-m_2^2}{2(m_1+m_2)}, \tag{2.37}$$

which is just the energy map between the relativistic energy $\mathcal{E}$ of a real two-body system and the relativistic energy $\mathcal{E}_0$ of the EOB system. This result is consistent to Eq. (1.6), which is also exactly the result obtained by Damour in the Ref. [16].

The 2nd order of I_R^0 is

$$\frac{G^2}{16J}\Big[(11-2a_2+b_2)\mathcal{E}^4+(11-2a_2+b_2)(m_1^4+m_2^4)-2(11-2a_2+b_2)\mathcal{E}^2(m_1^2+m_2^2)+2(13-2a_2-b_2)m_1^2m_2^2\Big]. \tag{2.38}$$

Correspondingly the second order of I_R is

$$\frac{G^2}{16J}\frac{15(m_1+m_2)}{\mathcal{E}}\Big[\mathcal{E}^4+(m_1^4+m_2^4)-2\mathcal{E}^2(m_1^2+m_2^2)+\frac{6}{5}m_1^2m_2^2\Big]. \tag{2.39}$$

Combining Eqs. (2.38) and (2.39), we obtain

$$\begin{aligned}11-2a_2+b_2&=\frac{15(m_1+m_2)}{\mathcal{E}},\\ 13-2a_2-b_2&=\frac{9(m_1+m_2)}{\mathcal{E}},\end{aligned} \tag{2.40}$$

which lead to

$$a_2 = \frac{6(\mathcal{E} - m_1 - m_2)}{\mathcal{E}}, \tag{2.41}$$

$$b_2 = \frac{\mathcal{E} + 3m_1 + 3m_2}{\mathcal{E}}. \tag{2.42}$$

From Eqs. (2.41) and (2.42), we can see that the effective metric at the 2PM order depends not only on m_1, m_2, but also on the relativistic energy $\mathcal{E}$ of the real binary system.Since $\mathcal{E}$ is determined by the initial configuration of the binary system and different initial configuration may yield different gravitational radiation, the above dependence just means the gravitational radiation depends on the initial configuration of the binary system. Therefore, we think such kind of effective metric is physically reasonable. As a special case, we consider the test particle limit of the behaviors of a_2 and b_2. For this purpose, by introducing the dimensionless ratio h

$$h := \frac{\mathcal{E}}{m_1 + m_2} - 1, \tag{2.43}$$

so that we have

$$a_2 = \frac{6h}{1+h}, \quad b_2 = \frac{4+h}{1+h}. \tag{2.44}$$

From the energy map (2.37), the dimensionless energy variable $\hat{\mathcal{E}}_{\rm eff} \equiv \frac{\mathcal{E}_0}{m_0}$ reads [38]

$$\hat{\mathcal{E}}_{\rm eff} = \frac{h^2 + 2h + 2\nu}{2\nu}, \tag{2.45}$$

then we obtain

$$h + 1 = \sqrt{1 + 2\nu(\hat{\mathcal{E}}_{\rm eff} - 1)}, \tag{2.46}$$

and from Eq. (2.44) one gets

$$a_2 = \frac{6\left(\sqrt{1 + 2\nu(\hat{\mathcal{E}}_{\rm eff} - 1)} - 1\right)}{\sqrt{1 + 2\nu(\hat{\mathcal{E}}_{\rm eff} - 1)}}, \tag{2.47}$$

$$b_2 = \frac{3 + \sqrt{1 + 2\nu(\hat{\mathcal{E}}_{\rm eff} - 1)}}{\sqrt{1 + 2\nu(\hat{\mathcal{E}}_{\rm eff} - 1)}}. \tag{2.48}$$

For the test particle limit ($\nu \to 0$), a_2 and b_2 reduce to

$$a_2 = 0, \quad b_2 = 4. \tag{2.49}$$

This result is consistent to the case that a test particle moving in the Schwarzschild spacetime since

$$\left(1 - \frac{GM_0}{R}\right)^{-1} = 1 + \frac{2GM_0}{R} + 4\left(\frac{GM_0}{R}\right)^2 + \mathcal{O}(G^3). \tag{2.50}$$

Back to the general case, if we work in the isotropic gauge and choose $\tilde{\beta}_1 = 1$, the energy map and effective metric can be obtained from Eqs. (2.15), (2.29), (2.31), (2.32) and (2.34). More precisely, direct calculation gives the energy map

$$\mathcal{E}_0 = \frac{\mathcal{E}^2 - m_1^2 - m_2^2}{2(m_1 + m_2)}. \tag{2.51}$$

It coincides with Eq. (2.37), the one obtained in Schwarzschild gauge, as we expected. Furthermore, the expansion coefficients in Eqs. (2.17) and (2.18) in the isotropic gauge can be deduced as

$$\tilde{a}_2 = \frac{2(4\mathcal{E} - 3m_1 - 3m_2)}{\mathcal{E}}, \tag{2.52}$$

$$\tilde{b}_2 = \frac{3(m_1 + m_2)}{2\mathcal{E}}. \tag{2.53}$$

3 Energy map and effective metric based on precession angle

Damour have studied the energy map between a real two-body system and the EOB system, by calculating the scattering angles, at the 1PM order [16]. Since here we focus on the bound states of a two-body system, the scattering angle should be replaced by the precession angle. In this section, we investigate the energy map and the effective metric at the 2PM order by analyzing the precession angles.

3.1 Precession angle of real two-body system at 2PM order

For a real two-body system, we have shown in Sect. 2 that the expression of p_r^2 at the 2PM order is

$$p_r^2 = \frac{P_0 r^2 - J^2}{r^2} + P_1\left(\frac{G}{r}\right) + P_2\left(\frac{G}{r}\right)^2, \tag{3.1}$$

where P_0, P_1, P_2 are given by Eqs. (2.8), (2.9) and (2.10).

For a general central-field Hamiltonian, $H(r, \vec{p}^2)$, the precession angle is given by

$$\psi = -2\pi + 2J\int_{r_1}^{r_2} \frac{dr}{r^2\sqrt{p_r^2}}, \tag{3.2}$$

where r_1 and r_2 are the roots of $p_r^2 = 0$, and from Eq. (3.1), they are given by

$$r_1 = \frac{-P_1 G + \sqrt{P_1^2 G^2 - 4P_0 P_2 G^2 + 4P_0 J^2}}{2P_0}, \tag{3.3}$$

and

$$r_2 = \frac{-P_1 G - \sqrt{P_1^2 G^2 - 4P_0 P_2 G^2 + 4P_0 J^2}}{2P_0}. \tag{3.4}$$

To calculate the precession angle, we first introduce a formula

$$\int_b^a \frac{1}{x\sqrt{-(x-b)(x-a)}} dx = \frac{\pi}{\sqrt{ab}}, \tag{3.5}$$

where $a > b > 0$. This formula may be proved directly, by transforming the variable from x to t,

$$t = \sqrt{\frac{a-x}{x-b}}, \tag{3.6}$$

and one then obtains

$$\begin{aligned}\int_b^a & \frac{1}{x\sqrt{-(x-b)(x-a)}}dx \\ &= \lim_{u\to b^+}\lim_{v\to a^-}\int_u^v \frac{1}{x(x-b)\sqrt{\frac{a-x}{x-b}}} \\ &= -\frac{2}{\sqrt{ab}}\left(0-\frac{\pi}{2}\right) = \frac{\pi}{\sqrt{ab}}.\end{aligned} \tag{3.7}$$

Using Eq. (3.5), the precession angle may be calculated as

$$\psi = -2\pi + 2J\int_{r_1}^{r_2}\frac{dr}{r^2\sqrt{p_r^2}} = P_2\pi\left(\frac{G}{J}\right)^2 + \mathcal{O}(G^3). \tag{3.8}$$

By inserting Eq. (2.10) into Eq. (3.8), the precession angle of a real two-body system at the 2PM order becomes

$$\begin{aligned}\psi = \frac{3(m_1+m_2)\pi}{8\mathcal{E}}\Big(&5\mathcal{E}^4 + 5m_1^4 + 5m_2^4 \\ &+6m_1^2m_2^2 - 10\mathcal{E}^2(m_1^2+m_2^2)\Big)\left(\frac{G}{J}\right)^2.\end{aligned} \tag{3.9}$$

It should be mentioned that one can also get the precession angle from the of scattering information [35], which gives the same result as above.

3.2 Precession angle of EOB system at the 2PM order

We now compute the effective precession angle ψ_0 in isotropic gauge ($C(R) = B(R)$). For an EOB system, we have obtained, in Sect. II, that

$$P_R^2 = \frac{dS_R^0}{dR} = \frac{B(R)}{c^2A(R)}\mathcal{E}_0^2 - B(R)\left(m_0^2c^2 + \frac{J_0^2}{C(R)R^2}\right), \tag{3.10}$$

where $A(R)$, $B(R)$ are given by Eqs. (2.17) and (2.18) with expansion coefficients $\tilde{a}_2$, $\tilde{\beta}_1$ and $\tilde{b}_2$.

Within isotropic coordinates, direct calculation shows that P_R^2 at the 2PM order is

$$P_R^2 = \frac{A_0R^2 - J_0^2}{R^2} + A_1\left(\frac{G}{R}\right) + A_2\left(\frac{G}{R}\right)^2, \tag{3.11}$$

where

$$\begin{aligned}A_0 &= \mathcal{E}_0^2 - m_0^2, \\ A_1 &= 2M_0(-m_0^2\tilde{\beta}_1 + \mathcal{E}_0^2(1+\tilde{\beta}_1)), \\ A_2 &= M_0^2(-\tilde{b}_2m_0^2 + \mathcal{E}_0^2(4-\tilde{a}_2+\tilde{b}_2+4\tilde{\beta}_1)).\end{aligned} \tag{3.12}$$

The zeros of P_R^2 are given by

$$R_1 = \frac{-A_1G + \sqrt{A_1^2G^2 - 4A_0A_2G^2 + 4A_0J_0^2}}{2A_0}, \tag{3.13}$$

and

$$R_2 = \frac{-A_1G - \sqrt{A_1^2G^2 - 4A_0A_2G^2 + 4A_0J_0^2}}{2A_0}. \tag{3.14}$$

From Eq. (3.5), the effective precession angle can be computed and the result is

$$\psi_0 = M_0^2\pi\Big(-\tilde{b}_2m_0^2 + \mathcal{E}_0^2(4-\tilde{a}_2+\tilde{b}_2+4\tilde{\beta}_1)\Big)\left(\frac{G}{J_0}\right)^2. \tag{3.15}$$

3.3 Effective metric at 2PM order based on precession angle

Now we construct the effective metric through identifying the effective scattering angle ψ_0 to the real two-body one ψ:

$$\psi_0(\mathcal{E}_0, J_0) = \psi(\mathcal{E}, J). \tag{3.16}$$

Recall that

$$\mathcal{E}_0 = \frac{\mathcal{E}^2 - m_1^2 - m_2^2}{2(m_1+m_2)},\ J_0 = J, \tag{3.17}$$

then Eq. (3.15) becomes

$$\begin{aligned}\psi_0 = \frac{G^2\pi}{4J^2}\Big[&(8-\tilde{a}_2+\tilde{b}_2)\mathcal{E}^4 + (8-\tilde{a}_2+\tilde{b}_2)(m_1^4+m_2^4) \\ &-2(8-\tilde{a}_2+\tilde{b}_2)\mathcal{E}^2(m_1^2+m_2^2) \\ &+(16-2\tilde{a}_2-2\tilde{b}_2)m_1^2m_2^2\Big],\end{aligned} \tag{3.18}$$

where we have used Eqs. (2.31), (2.32) and $\tilde{\beta}_1 = 1$. By noticing that Eq. (3.9) can be rewritten as

$$\begin{aligned}\psi = \frac{15(m_1+m_2)\pi G^2}{8\mathcal{E}J^2}\Big[&\mathcal{E}^4 + (m_1^4+m_2^4) \\ &-2\mathcal{E}^2(m_1^2+m_2^2) + \frac{6}{5}m_1^2m_2^2\Big],\end{aligned} \tag{3.19}$$

and from Eqs. (3.16), (3.18) and (3.19), we obtain

$$\begin{aligned}8-\tilde{a}_2+\tilde{b}_2 &= \frac{15(m_1+m_2)}{2\mathcal{E}}, \\ 16-2\tilde{a}_2-2\tilde{b}_2 &= \frac{9(m_1+m_2)}{\mathcal{E}},\end{aligned} \tag{3.20}$$

which lead to

$$\begin{aligned}\tilde{a}_2 &= \frac{2(4\mathcal{E}-3m_1-3m_2)}{\mathcal{E}}, \\ \tilde{b}_2 &= \frac{3(m_1+m_2)}{2\mathcal{E}}.\end{aligned} \tag{3.21}$$

This is consistent with Eqs. (2.52) and (2.53).

4 Comparison with existing results

In the Schwarzschild gauge, we have shown that the effective metric is

$$ds^2_{\rm eff} = -A(R)dt^2 + B(R)dR^2 + C(R)R^2(d\Theta^2 + \sin^2\Theta d\Phi^2), \tag{4.1}$$

with

$$A(R) = 1 - \frac{2GM_0}{R} + a_2\left(\frac{GM_0}{R}\right)^2, \tag{4.2}$$

$$B(R) = 1 + \frac{2GM_0}{R} + b_2\left(\frac{GM_0}{R}\right)^2, \tag{4.3}$$

where

$$a_2 = \frac{6(\mathcal{E} - m_1 - m_2)}{\mathcal{E}} = \frac{6(\sqrt{1+2\nu(\hat{\mathcal{E}}_{\rm eff}-1)}-1)}{\sqrt{1+2\nu(\hat{\mathcal{E}}_{\rm eff}-1)}},$$
$$b_2 = \frac{\mathcal{E} + 3m_1 + 3m_2}{\mathcal{E}} = \frac{3+\sqrt{1+2\nu(\hat{\mathcal{E}}_{\rm eff}-1)}}{\sqrt{1+2\nu(\hat{\mathcal{E}}_{\rm eff}-1)}}. \tag{4.4}$$

For later convenience, we introduce the following dimensionless quantities [38]

$$p_\mu = \frac{P_\mu}{m_0},\ u = \frac{1}{r} = \frac{GM}{R}, \tag{4.5}$$

so that, at the 2PM order, a_2 and b_2 can be rewritten as

$$a_2 = \frac{6\left(\sqrt{1+2\nu(\hat{H}_{\rm Schw}-1)}-1\right)}{\sqrt{1+2\nu(\hat{H}_{\rm Schw}-1)}}, \tag{4.6}$$

$$b_2 = \frac{3+\sqrt{1+2\nu(\hat{H}_{\rm Schw}-1)}}{\sqrt{1+2\nu(\hat{H}_{\rm Schw}-1)}}, \tag{4.7}$$

where $\hat{H}_{\rm Schw}$, the reduced effective Hamiltonian of a test particle moving in a Schwarzschild background, is given by [38],

$$\hat{H}^2_{\rm Schw} = (1-2u)\left(1 + (1-2u)p_r^2 + p_\varphi^2 u^2\right). \tag{4.8}$$

Moreover, the squared reduced effective Hamiltonian $\hat{\mathcal{E}}^2_{\rm eff} = \frac{\mathcal{E}^2_0}{m_0^2}$ at the 2PM order reads

$$\hat{\mathcal{E}}^2_{\rm eff} = (1 - 2u + a_2u^2)\left(1 + \frac{p_r^2}{1+2u+b_2u^2} + p_\varphi^2u^2\right). \tag{4.9}$$

In the following, we compare our 2PM effective Hamiltonian to the corresponding PN-expanded effective Hamiltonian at 3PN accuracy analytically and compare our 2PM Hamiltonian to the existing 2PM Hamiltonian obtained in the Ref. [38].

4.1 Comparison with existing 3PN result

We use $\hat{\mathcal{E}}^2_{\rm eff} - 1$ as PN expansion parameter. At the 3PN accuracy,

$$\hat{H}_{\rm Schw} - 1 = \frac{1}{2}(\hat{H}^2_{\rm Schw} - 1) - \frac{1}{8}(\hat{H}^2_{\rm Schw} - 1)^2 + \mathcal{O}((\hat{H}^2_{\rm Schw} - 1)^3), \tag{4.10}$$

and then

$$\begin{aligned} a_2 &= 6\left(1 - \frac{1}{\sqrt{1+2\nu(\hat{H}_{\rm Schw}-1)}}\right) \\ &= 6\nu(\hat{H}_{\rm Schw}-1) - 9\nu^2(\hat{H}_{\rm Schw}-1)^2 + \mathcal{O}((\hat{H}_{\rm Schw}-1)^3) \\ &= 3\nu(\hat{H}^2_{\rm Schw}-1) - \left(\frac{3\nu}{4} + \frac{9\nu^2}{4}\right)(\hat{H}^2_{\rm Schw}-1)^2 + \mathcal{O}((\hat{H}^2_{\rm Schw}-1)^3), \end{aligned} \tag{4.11}$$

$$\begin{aligned} b_2 &= 1 + \frac{3}{\sqrt{1+2\nu(\hat{H}_{\rm Schw}-1)}} \\ &= 4 - \frac{3}{2}\nu(\hat{H}^2_{\rm Schw}-1) + \frac{3}{8}(\nu+3\nu^2)(\hat{H}^2_{\rm Schw}-1)^2 + \mathcal{O}((\hat{H}^2_{\rm Schw}-1)^3). \end{aligned} \tag{4.12}$$

By substituting Eqs. (4.11), (4.12) and (4.8) into the Eq. (4.9), we obtain the squared reduced effective Hamiltonian at "2PM+3PN" order as

$$\begin{aligned} (\hat{\mathcal{E}}^{\rm 2PM+3PN}_{\rm eff})^2 = (1-2u)\Big[&1 + (1-2u+3\nu u^2)p_r^2 \\ &+ (1+3\nu u^2)p_\varphi^2u^2\Big] \\ &+ \Big[\frac{15}{4}p_r^4 + 3p_r^2p_\varphi^2u^2 - \frac{3}{4}p_\varphi^4u^4 \\ &- \frac{9\nu}{4}(p_r^4 + 2p_r^2p_\varphi^2u^2 + p_\varphi^4u^4)\Big]\nu u^2. \end{aligned} \tag{4.13}$$

On the other hand, the 3PN effective Hamiltonian is given by [13]

$$(\hat{\mathcal{E}}^{\rm 3PN}_{\rm eff})^2 = A(u')\left(1 + \frac{A(u')}{D(u')}p_r'^2 + p_\varphi'^2u'^2\right) + z_3u'^2p_r'^4, \tag{4.14}$$

where

$$A(u') = 1 - 2u' + 3\nu u'^3 + \left(\frac{94}{3} - \frac{41}{32}\pi^2 + 2\omega_{\text{static}}\right)\nu u'^4, \tag{4.15}$$

$$D(u') = 1 - 6\nu u'^2 + 2(3\nu - 26)\nu u'^3, \tag{4.16}$$

$$z_3 = 2(4 - 3\nu)\nu. \tag{4.17}$$

At "3PN+2PM" accuracy,

$$(\hat{\mathcal{E}}_{\text{eff}}^{\text{3PN+2PM}})^2 = (1 - 2u')\Big[1 + p_r'^2(1 - 2u' + 6\nu u'^2) + p_\varphi'^2 u'^2\Big] + (8\nu - 6\nu^2)u'^2 p_r'^4. \tag{4.18}$$

In order to check the consistence between Eqs. (4.13) and (4.18), we take a canonical transformation

$$q'^i = q^i + \frac{\partial g(q, p')}{\partial p_i'}, \tag{4.19}$$

$$p_i = p_i' + \frac{\partial g(q, p')}{\partial q^i}. \tag{4.20}$$

One can show directly that Eqs. (4.13) and (4.18) are consistent to each other at 2PM and 3PN accuracy by choosing the canonical generating function as

$$g(q, p') = p_r'\left(-\frac{3\nu}{2r} - \frac{(13 - 9\nu)\nu p_\varphi'^2}{8r^3} - \frac{1}{8}(17 - 15\nu)\nu\frac{p_r'^2}{r}\right). \tag{4.21}$$

This implies our 2PM effective Hamiltonian is consistent to the existing result at 3PN accuracy.

4.2 Comparison to the existing results

In this subsection, we compare our EOB predictions for the binding energy of a two body system on a quasi-circular orbit to the results of existing PM EOB models [38,39]. To this end, we introduce

$$e \equiv \frac{E - M}{m_0}, \quad l \equiv \frac{L}{GMm_0}, \tag{4.22}$$

where E and L are the total energy and angular momentum of a two-body system, and use adiabatic approximation [39] to investigate the energy-angular momentum relation.

We compare the e-l relation for previous PM EOB Hamiltonian to our new PM EOB Hamiltonian in Fig. 1. Our 1PM EOB behaves exactly the same as Damour's 1PM result. Damour's 2PM EOB Hamiltonian used Finsler-type corrections. Our new 2PM EOB Hamiltonian does not use Finsler-type corrections. Along with a binary evolves from inspiral to merger, l decrease and the difference increases. When l goes to l_{ISCO} [39], the relative deviation of binding energy increases to about 1%. At the mean time we note that 1PM result is even closer to 3PM result than 2PM results. We blame this behavior to the nonmonotonic convergence of PM expansion. Due to this reason, we can not judge whether our 2PM result or Damour's 2PM result is more accurate. More investigation on the PM approximated EOB theory is needed.

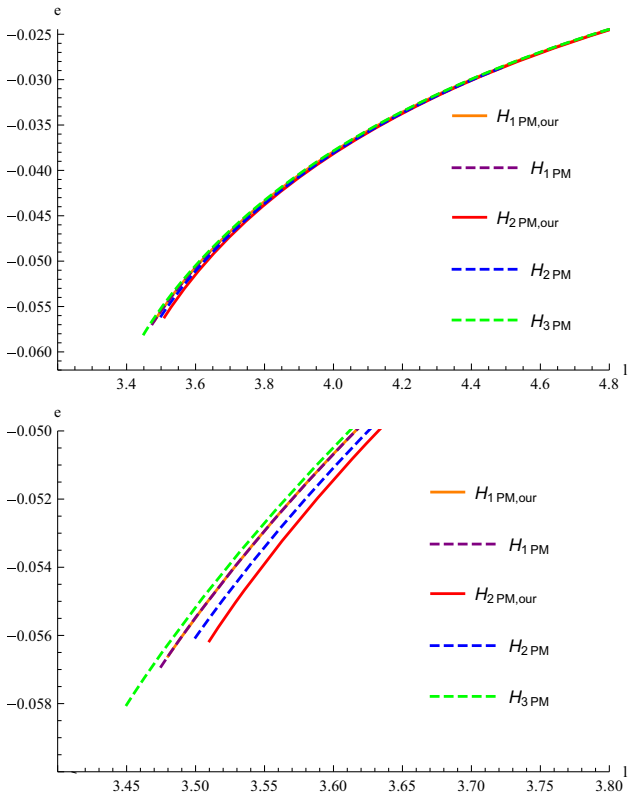

Fig. 1 The above plot shows the energetics of different EOB Hamiltonians. $H_{\text{1PM,our}}$ and $H_{\text{2PM,our}}$ mean the 1PM and 2PM results got in the current work. H_{1PM} [38], H_{2PM} [38] and H_{3PM} [39] are the existing results. The bottom plot corresponds to the zooming in for the $l \in (3.45, 3.65)$ range

5 Summary and discussion

The EOB formalism is a successful theory to investigate the gravitational radiation emitted by binary black holes. Combined with the results of numerical relativity, the EOBNR model has been developed and has played an important role in the analysis of the gravitational wave signals. The seminal EOB theory is based on the knowledge of a PN description of the relativistic two-body dynamics. The PM approach is another useful approximation method to deal with the relativistic two-body problem. Recently, Damour et al. began to construct the EOB theory based on the PM approximation. At the 1PM order, by identifying the scattering angle of the scattering states of a real two-body system and the effective one [16], the energy map between the relativistic energy

of real two-body system and the one of effective one-body system takes form

$$\frac{\mathcal{E}_0}{m_0} = \frac{\mathcal{E}^2 - m_1^2 - m_2^2}{2m_1 m_2}. \tag{5.1}$$

In 2018, Damour found the 2PM Hamiltonian based on the calculation of scattering angle of the effective one-body system by using a generalized mass-shell condition which contains a Finsler-type contribution [38]. Antonelli et al extended Damour's results to the 3PM order and discussed the energetics of two-body Hamiltonians in the 3PM accuracy [39].

In this work, we investigate the energy map, the effective metric and the effective Hamiltonian in the EOB theory at the second PM approximation based on a quite different scheme. We calculate the radial action variables and precession angles for bound states, and show that the energy map (5.1) is still valid for a two-body problem at the 2PM order. Furthermore, we construct the effective metric within EOB formalism at the 2PM order based on the action variable method and precession method respectively, and observe that both methods give the same results. When we calculate the effective metric, we do not take any other extra assumptions besides the PM approximation. This is different to Damour's work where a Finsler-type contribution is assumed. Our effective metric at the 2PM order depends on the relativistic energy $\mathcal{E}$ of the real binary system, which is physically reasonable because different $\mathcal{E}$ corresponds to different initial configuration of the binary system and different initial configuration may result in different gravitational radiation. In addition, we compare our 2PM effective Hamiltonian with the existing results and find they are consistent with each other at the 3PN accuracy.

In this paper, we extend Damour's discussion on effective one-body theory (based on PM approximation) from scattering states to bound states. Our derivation is based on the direct investigation of a bound state, and we give the effective metric explicitly which is useful to further investigate gravitational waves produced by a binary system. In the next step we would like to construct the energy map and effective metric to higher-order PM approximation and to generalize the framework obtained in this work to a binary system with spin.

Acknowledgements We thank S. Chen and Q. Pan for many useful discussions and comments on the manuscript. J. Jing was supported by the Grant of NSFC nos. 12035005, 11875025. X. He was supported by the Grant of NSF of Hunan province no. 2018JJ2073. Z. Cao was supported by the NSFC (no. 11690023 and no. 11920101003).

Data Availability Statement This manuscript has no associated data or the data will not be deposited. [Authors' comment: All related data have published in the paper.]

Open Access This article is licensed under a Creative Commons Attribution 4.0 International License, which permits use, sharing, adaptation, distribution and reproduction in any medium or format, as long as you give appropriate credit to the original author(s) and the source, provide a link to the Creative Commons licence, and indicate if changes were made. The images or other third party material in this article are included in the article's Creative Commons licence, unless indicated otherwise in a credit line to the material. If material is not included in the article's Creative Commons licence and your intended use is not permitted by statutory regulation or exceeds the permitted use, you will need to obtain permission directly from the copyright holder. To view a copy of this licence, visit http://creativecommons.org/licenses/by/4.0/.
Funded by SCOAP[3].

References

1. B.P. Abbott et al., LIGO Scientific and Virgo Collaborations. Phys. Rev. Lett. **116**, 061102 (2016)
2. B.P. Abbott et al., LIGO Scientific and Virgo Collaborations. Phys. Rev. Lett. **116**, 241103 (2016)
3. B.P. Abbott et al., LIGO Scientific and Virgo Collaborations. Phys. Rev. Lett. **118**, 221101 (2017)
4. B.P. Abbott et al., LIGO Scientific and Virgo Collaborations. Phys. Rev. Lett. **119**, 141101 (2017)
5. B.P. Abbott et al., LIGO Scientific and Virgo Collaborations. Phys. Rev. Lett. **119**, 161101 (2017)
6. B.P. Abbott et al., LIGO Scientific and Virgo Collaborations. Phys. Rev. X **9**, 031040 (2019)
7. R. Cai, Z. Cao, Z. Guo, Natl. Sci. Rev. **4**, 687 (2017)
8. Z. Cao, B. Han, Phys. Rev. D **96**, 044028 (2017)
9. A. Buonanno, Y. Pan, J.G. Baker, J. Centrella, B.J. Kelly, S.T. McWilliams, J.R. van Meter, Phys. Rev. D **76**, 104049 (2007)
10. A. Taracchini, A. Buonanno, Y. Pan, T. Hinderer, M. Boyle, D.A. Hemberger, L.E. Kidder, G. Lovelace, A.H. Mroué, H.P. Pfeiffer et al., Phys. Rev. D **89**, 061502 (2014)
11. A. Buonanno, T. Damour, Phys. Rev. D **59**, 084006 (1999)
12. A. Buonanno, T. Damour, Phys. Rev. D **62**, 064015 (2000)
13. T. Damour, P. Jaranowski, G. Schafer, Phys. Rev. D **62**, 084011 (2000)
14. T. Damour, Phys. Rev. D **64**, 124013 (2001)
15. T. Damour, P. Jaranowski, G. Schafer, Phys. Rev. D **91**, 084024 (2015)
16. T. Damour, Phys. Rev. D **94**, 104015 (2016)
17. B. Bertotti, Nuovo Cimento **4**, 898 (1956)
18. B. Bertotti, J. Plebanski, Ann. Phys. **11**, 169 (1960)
19. D. Bini, T. Damour, Phys. Rev. D **96**, 104038 (2017)
20. D. Bini, T. Damour, Phys. Rev. D **98**, 044036 (2018)
21. T. Damour, Phys. Rev. D **102**, 024060 (2020)
22. D. Bini, T. Damour, A. Geralico, Phys. Rev. D **101**, 044039 (2020)
23. G. He, W. Lin, Phys. Rev. D **94**, 063011 (2016)
24. G. He, W. Lin, Class. Quantum Gravity **34**, 105006 (2017)
25. L. Blanchet, A. Fokas, Phys. Rev. D **98**, 084005 (2018)
26. J. Vines, Class. Quantum Gravity **35**, 084002 (2018)
27. C. Cheung, I. Rothstein, M. Solon, Phys. Rev. Lett. **121**, 251101 (2018)
28. J. Vines, J. Steinhoff, A. Buonnanno, Phys. Rev. D **99**, 064054 (2019)
29. A. Cristofoli, N. Bjerrum-Bohr, P. Damgaard, P. Vanhove, Phys. Rev. D **100**, 084040 (2019)
30. A. Collado, P. Vecchia, R. Russo, Phys. Rev. D **100**, 066028 (2019)
31. Z. Bern, C. Cheung, R. Robin, C.H. Shen, M.P. Solon, M. Zeng, Phys. Rev. Lett. **122**, 201603 (2019)
32. Z. Bern, C. Cheung, R. Robin, C.H. Shen, M.P. Solon, M. Zeng, JHEP **10**, 206 (2019)
33. J. Plefka, C. Shi, J. Steinhoff, T. Wang, Phys. Rev. D **100**, 086006 (2019)
34. G. Kalin, R.A. Porto, JHEP **01**, 072 (2020)

35. G. Kalin, R.A. Porto, JHEP **02**, 120 (2020)
36. C. Cheung, M. Solon, Phys. Rev. Lett. **125**, 191601 (2020)
37. S. Roy, R. Koley, P. Majumdar, Phys. Rev. D **102**, 084045 (2020)
38. T. Damour, Phys. Rev. D **97**, 044038 (2018)
39. A. Antonelli, A. Buonanno, J. Steinhoff, M. van de Meent, J. Vines, Phys. Rev. D **99**, 104004 (2019)
40. T. Damour, G. Schafer, Nuovo Cimento **10**, 123 (1988)